Russian Physics Journal, Vol. 48, No. 9, 2005

PHYSICS OF MAGNETIC PHENOMENA

IR AND NMR SPECTRA OF CRYSTALLINE AND AMORPHOUS COPPER METABORATE

G. A. Petrakovskii, L. V. Udod, K. A. Sablina, Yu. N. Ivanov, A. Ya. Korets, and A. F. Bovina

UDC 535.343.2: 539.14.43

IR and NMR spectroscopic investigations of crystalline and amorphous copper metaborate CuB_2O_4 *as well as of copper metaborate crystallized from the amorphous state have been carried out for the first time. For an amorphous sample, a new wide absorption band arises in the frequency range ~1200–1600 cm*$^{-1}$*. This band is due to conversion of a number of tetrahedral* BO_4 *units of the crystalline sample into the trigonal* BO_3 *units. The presence of trigonal units in amorphous* CuB_2O_4 *is confirmed by the* ^{11}B *NMR spectra. Based on the data of IR and NMR spectroscopy, significant intensification of the exchange interaction is explained by the formation of shorter exchange bridges during amorphyzation of* CuB_2O_4.

INTRODUCTION

The congruent character of melting of $CuGeO_3$, Bi_2CuO_4, and CuB_2O_4 oxocuprites and the presence of classical B_2O_3 and conditional GeO_2 and Bi_2O_3 glassformers in these compounds give a unique opportunity to translate these compounds into the amorphous state and to investigate the influence of amorphyzation on the magnetic properties of the substance comparing these properties in crystalline and amorphous states [1–3].

The magnetic and resonant properties of crystalline and amorphous CuB_2O_4 were measured in [3]. Amorphyzation significantly changed the magnetic properties of copper metaborate. Intensification of antiferromagnetic interaction, deviation from the Curie–Weiss law below 40 K, and anomalous temperature dependences of the magnetic susceptibility and resonant parameters at $T \sim 8$ K were established. A conclusion was made about the formation of shorter exchange bridges that explained the observed changes in the magnetic properties of amorphous CuB_2O_4.

Exchange interactions between Cu^{2+} ions ($S = 1/2$) in CuB_2O_4 crystal are realized through the long Cu–O–B–O–Cu bridges incorporating boron ions [3]. Copper cations in CuB_2O_4 occupy two nonequivalent positions. This causes the formation of two magnetic subsystems, one of which is three-dimensional and is ordered at $T_N = 20$ K, whereas the second is formed by zigzag chains of copper ions with frustrated exchange bonds with the first subsystem [4]. The exchange between chains is also frustrated and weak. The coexistence of these two subsystems with different magnetic dimensions and degrees of magnetic ordering predetermines rich and complex phase diagrams of the magnetic state of copper metaborate [5, 6]. In the CuB_2O_4 crystal, there are boron ions of two types four-fold coordinated by oxygen atoms but with different B–O distances. These BO_4 tetrahedrons are bonded by oxygen ions and form a three-dimensional network of metaborate rings comprising $(B_3O_6)^{3-}$ units. All boron and oxygen atoms take part in many indirect exchange bonds with numerous neighbors. Thus, the copper ions of the first subsystem have 24 indirect bonds with 16 neighbors each, and the copper ions of the second subsystem have 24 bonds with 14 neighbors each. This suggests that the entire boron-oxygen core participates in the CuB_2O_4 exchange interaction.

L. V. Kirenskii Institute of Physics of the Siberian Branch of the Russian Academy of Sciences, e-mail: luba@iph.krasn.ru. Translated from Izvestiya Vysshikh Uchebnykh Zavedenii, Fizika, No. 9, pp. 73–78, September, 2005. Original article submitted June 30, 2005.

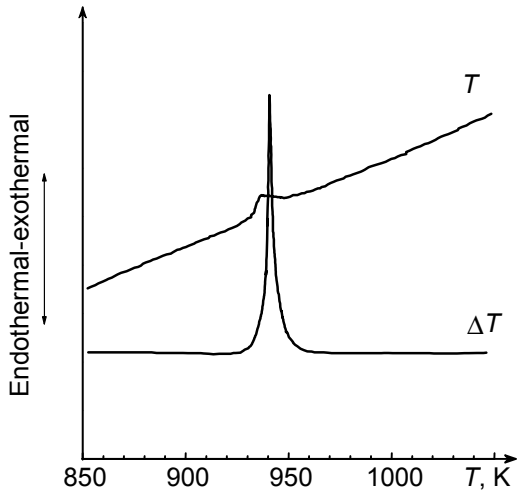

Fig. 1. Data of differential thermal analysis of amorphous CuB_2O_4.

By now, beginning with [7, 8], a large body of information on physical and chemical properties of crystalline and glassy systems containing boron oxide B_2O_3 has been collected. Results of these investigations testify to the presence of large borate groups in boron-containing oxide compounds in the glassy state; they either remain unchanged during vitrification or are converted into anion groups with different coordination numbers. Moreover, both large borate groups are incorporated into the 3-D disordered network [9]. The conversion of boron-oxygen groups during CuB_2O_4 amorphyzation can cause the transformation of exchange bridges bonding the neighboring copper ions and hence can affect the exchange interaction pattern in glass.

To investigate structural changes of the boron-oxygen core in CuB_2O_4 during amorphyzation, we carried out IR spectral investigations in the frequency range ~(400–4000) cm^{-1} typical of the fundamental oscillations of borate anions of different structures [10]. To this end, we also investigated the ^{11}B (with a natural content of 80% and a quadrupole moment) NMR spectra of crystalline and amorphous CuB_2O_4 powders. It is well known that the NMR spectra of quadrupole nuclei are sensitive even to small structural changes in the examined substances and give information on the value and symmetry of intracrystal electric field gradients at the nucleus location.

PREPARATION OF SAMPLES

The CuB_2O_4 single crystals of bright blue-violet color were grown from the solution-melt by the spontaneous crystallization method [11]. Amorphous copper metaborate CuB_2O_4 was produced by fast pouring of the melt on a metal substrate. Diffusion scattering typical of the amorphous state was seen in the x-ray photographs of the powder prepared by grinding of peaces of the quenched melt. The x-ray photographs were taken using the DRON-2 facility (CuK_α radiation). In addition to the x-ray analysis, the differential thermal analysis was used to confirm the amorphous state of the sample.

Figure 1 shows a derivatogram of amorphous CuB_2O_4. At 930 K, the onset of exothermic glass crystallization was observed; it was accompanied by heat liberation. Repeated heating of this sample did not reveal exopeaks. This confirms first, the amorphous state of the sample and second, glass-crystal direction of the phase transition on heating of amorphous CuB_2O_4. The color of the powder changed from initial black to green and further to blue-violet with increasing exposure time at a temperature of 950 K. The x-ray analysis of the powder after heat treatment at 950 K revealed all most typical lines of crystalline CuB_2O_4.

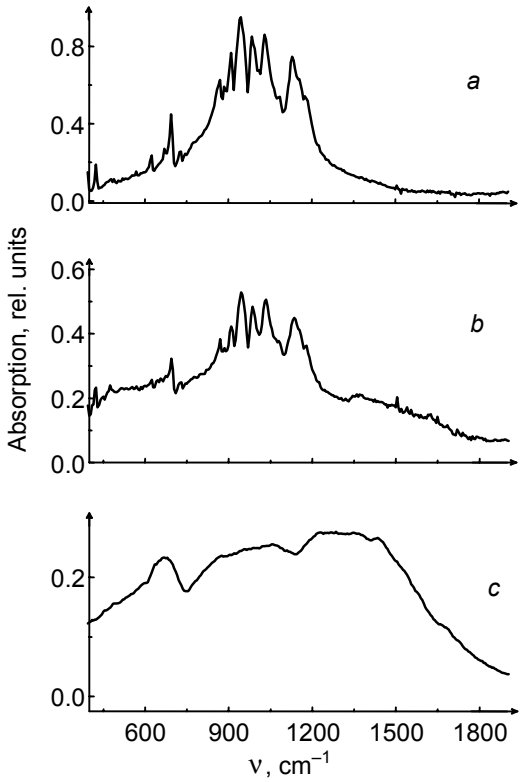

Fig. 2. IR absorption spectra of CuB_2O_4 for a) crystalline sample, b) sample crystallized from the amorphous state, and c) amorphous sample.

IR AND NMR INVESTIGATIONS

Optical measurements were performed using a Specord M-82 two-beam IR spectrometer by the transmitted radiation absorption method at room temperature. Samples shaped as tablets were prepared by pressing of powders in the KBr matrix.

Figure 2 shows the IR spectra of three samples. The IR spectrum of crystalline CuB_2O_4 shown in Fig. 2*a* completely coincides with the IR spectrum in the frequency range ~400–2000 cm^{-1} presented in [12]. Because there are tetrahedrons of two types constructed from boron atoms coordinated by oxygen in the crystal and all B–O bonds in the tetrahedrons of both types are nonequivalent because of distortions [13], the IR spectra contain a number of absorption lines. They are located mainly in the frequency range ~800–1200 cm^{-1}.

The smeared and broadened IR spectra of amorphous CuB_2O_4 in Fig. 2*b* are typical of the amorphous state of the substance. This is due to the disorder in the boron-oxygen network and even severer distortion of the local structure. Despite the spectra are smeared, a new absorption band in the frequency range ~1200–1600 cm^{-1} is clearly seen. If we conditionally subdivide the entire absorption frequency range into two parts: ~800–1200 cm^{-1} and ~1200–1600 cm^{-1}, with allowance for the intensities we can conclude that the initial band in the range ~800–1200 cm^{-1}, typical of crystalline CuB_2O_4, remained in the same frequency range, and the new band in the range ~1200–1600 cm^{-1} is caused by the conversion of some oscillations from the frequency range ~800–1200 cm^{-1}. This testifies to the significant structural reorganization during amorphyzation of CuB_2O_4.

After long-term heating at 950 K, the amorphous sample becomes crystalline. The IR spectrum of this sample is shown in Fig. 2*b*. The relative line intensities and positions in the IR spectra of CuB_2O_4 crystallized from the amorphous state and of its crystalline analogue coincide. Some traces of the amorphous state during crystallization of the sample, which

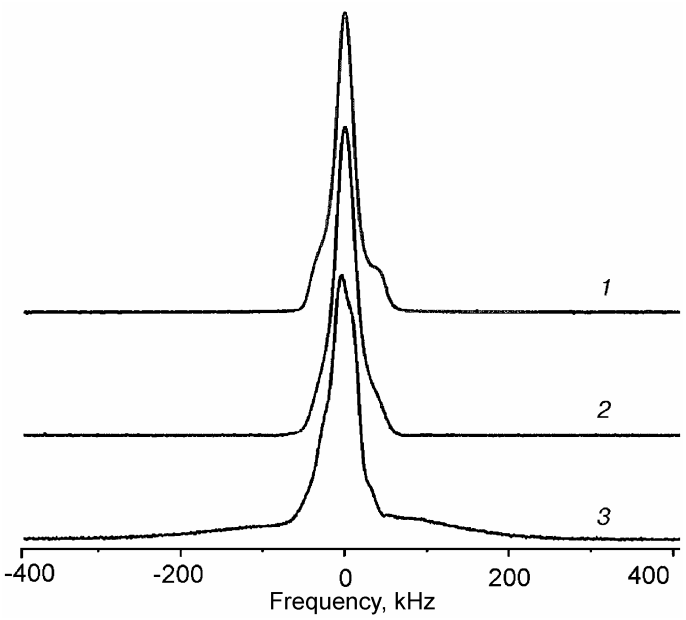

Fig. 3. NMR spectra of the CuB_2O_4 samples. Here curve *1* is for the crystalline sample, curve *2* is for the sample crystallized from the amorphous state, and curve *3* is for the amorphous state.

becomes less pronounced with increasing crystallization time, can be seen in the frequency range of the new absorption band for the amorphous sample.

The ^{11}B NMR spectra were registered using the BRUKER AVANCE-300 pulsed spectrometer at a frequency of 96.3 MHz at room temperature. The 90°-pulse duration was about 3.5 μs. To eliminate the influence of the dead time of the receiver of the NMR spectrometer, the spin-echo pulse train with 18-μs period between pulses was used. The ^{11}B nuclei have spins of 3/2 and hence quadrupole moments. A resonance on the nuclei with quadrupole moments gives information on the value and symmetry of intracrystal electric field gradients at the nucleus location.

In a strong external magnetic field $\boldsymbol{B}_0$, when the Zeeman interaction energy considerably exceeds the energy of interaction of the quadrupole moment of the nucleus with the intracrystal field, this intracrystal field causes perturbations of the equidistant Zeeman energy levels and splitting of NMR lines into $2I$ (I is the nucleus spin) components symmetric about the Larmor precession frequency. Hence, the ^{11}B NMR spectra consist of triplets with intensities in the ratios 2 : 3 : 2 whose number for the single crystal sample is determined generally by the number of magnetically nonequivalent ^{11}B nuclei. The quadrupole interaction intensity depends on the sample orientation in the field $\boldsymbol{B}_0$. Individual crystallites in the crystalline powder have every possible orientations in the magnetic field, so that the NMR spectra are averaged over orientations of the vector $\boldsymbol{B}_0$. They assume characteristic shapes of symmetric "tents." With increase in the electric field gradient, the intensity of tent wings sharply decreases, and only the central component (corresponding to the transition with $m = 1/2 \leftrightarrow -1/2$ and becoming asymmetric because of the influence of the second-order effects) often remains in actual NMR spectra of powders. High sensitivity of the ^{11}B NMR method to changes in the local symmetry of boron nuclei is often used to estimate the fraction N_4 of the 4-coordinated boron atoms in borate glasses [8].

The ^{11}B NMR spectrum of the CuB_2O_4 crystal powder is shown by curve *1* in Fig. 3. The central symmetric part of the spectrum belongs to the boron nuclei occupying positions with a higher symmetry (and hence with a lower electric field gradient). The asymmetric wide part of the NMR spectrum has the characteristic shape of the central NMR line in the presence of the second-order quadrupole effects. From the relative intensity of the NMR spectrum components it follows that the number of boron nuclei in one structurally nonequivalent position is twice as large as the number of boron nuclei in the other position. These results are in agreement with the structural data for CuB_2O_4 reported in [12, 13].

Curve *3* in Fig. 3 shows the NMR spectrum of amorphous CuB_2O_4. It also comprises two components: narrow and wide. The half-width and the shape of the narrow components changed only slightly in comparison with the polycrystalline

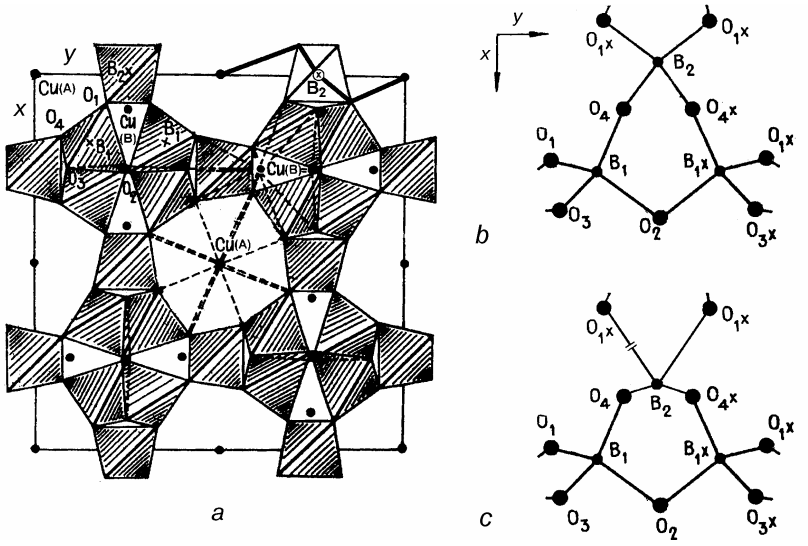

Fig. 4. Crystalline structure of CuB_2O_4 [13]: a) projection of the structure onto the (001) plane, b) general view of the $[B_3O_6]^{3-}$ radical in the projection onto the *xy* plane, and c) suggested pattern of tetrahedron conversion.

sample. The wide asymmetric component demonstrates a significant increase in the electric field gradient and hence essential changes in the nearest environment of the fraction of boron atoms in the amorphous sample. The relative intensity of the wide component is about 30%. As already indicated above, the boron-oxygen core of CuB_2O_4 is formed by the metaborate ring groups comprising three tetrahedrons each (Fig. 4). From the NMR data it follows that one third of tetrahedrons in glassy copper metaborate is subjected to severe distortion. At the same time, comparatively small changes of the central part of the NMR spectrum demonstrate that the remaining two thirds of tetrahedrons remain virtually unchanged.

Curve *2* in Fig. 3 shows the ^{11}B NMR spectrum of the sample crystallized from amorphous CuB_2O_4. As can be seen from the figure, it almost completely coincides with the spectrum of the crystalline sample (curve *1* in Fig. 3). Small differences are most likely due to the presence of a small amount of the impurity – amorphous CuB_2O_4 – in the crystallized sample.

DISCUSSION OF RESULTS

Among the problems of elucidation of the influence of amorphyzation on the CuB_2O_4 magnetic properties are an increase in the paramagnetic Curie temperature ($\Theta_\perp = -23$ K and $\Theta_\parallel = -17$ K for crystalline CuB_2O_4 and $\Theta = -56$ K for amorphous CuB_2O_4) and anomalous temperature dependences of the susceptibility and resonant characteristics [3].

The assumption on changes in the Cu–O–B–O–Cu exchange bridge during amorphyzation of CuB_2O_4 was made in [3]. In the present work it is demonstrated using the IR and NMR methods that these changes occur during amorphyzation. The frequencies of valence B–O oscillations in the IR spectra of crystal and amorphous states differ significantly. From the numerous literature data on the IR absorption of crystalline and glassy borate oxide compounds it follows that vibrational frequencies of B–O structures are active in the IR frequency range ~500–2000 cm^{-1} (for example, see [9, 10]). The absorption frequency range ~800–1200 cm^{-1} is typical of the antisymmetric valence B–O vibrations of the tetrahedral BO_4 units (tetrahedrons), while the higher-frequency absorption band in the range ~1200–1550 cm^{-1} is caused by the valence B–O vibrations of the trigonal BO_3 units (triangles). As to the frequency range ~600–800 cm^{-1}, it is typical of the metaborate ring groups [14].

Thus, the IR spectra vividly demonstrate that a fraction of tetrahedrons BO_4 is converted into the trigonal BO_3 units during amorphyzation of CuB_2O_4. According to [15], this more often occurs by breaking of the B–O bond and forming non-bridge oxygen. In [15] it was demonstrated that in xCuO$(50 - x)$PbO·$50B_2O_3$ glasses, BO_3 with one non-bridge oxygen has

two bands centered at 1235 and 1400 cm^{-1}. Unfortunately, these bands were masked by the wide absorption band in our IR spectrum, but their presence around 1210 and 1410 cm^{-1} can be judged with a sufficient degree of reliability from Fig. 2*c*. In [15] it was proved that when Pb in substituted by Cu, the fraction of triangles BO_3 decreases due to the formation of BO_4 units in metaborate ring groups with one non-bridge oxygen. In our case, metaborate rings were also observed.

From the ^{11}B NMR spectra of crystal copper metaborate (curve *1* in Fig. 3) it follows that boron nuclei occupy two structurally nonequivalent positions. The central part of the spectrum – the symmetric line with a half-width of about 27 kHz – is typical of the boron nuclei in the symmetric BO_4 groups. The wide component of the spectrum has the shape of the central NMR line for the axially symmetric tensor of the electric field gradient in the presence of the second-order quadrupole effects. Small splitting between the peaks of this component did not allow us to measure precisely the quadrupole coupling constant and testified to small distortions of the BO_4 groups of the second type in crystalline CuB_2O_4.

A comparison between the ^{11}B NMR spectra of crystalline (curve *1* in Fig. 3) and amorphous copper metaborate (curve *3* in Fig. 3) demonstrates that the parameters of the central line of the spectrum of amorphous CuB_2O_4 virtually coincide with those of the crystalline sample. Small changes in the central line profile in the spectrum of amorphous copper metaborate are due to weak distortions of the tetrahedral BO_4 groups and the absence of long-range crystalline order. The wide asymmetric line (its half-width exceeds 240 kHz) in the spectrum of amorphous CuB_2O_4 testifies to a significant increase in the electric field gradient (the quadrupole coupling constant increased almost by an order of magnitude) of a fraction of boron atoms in the amorphous sample. From a comparison of line intensities it follows that the nearest environment of approximately one third of the boron atoms has changed in the glassy sample. Such changes of the quadrupole interactions occur when the local symmetry of the nucleus position is reduced; they were observed in glassy B_2O_3 comprising the triangular BO_3 groups [16, 17]. However, in this case the tensor of the electric field gradient remained axially symmetric. More complex profile of the wide spectral component is indicative of the random distortions of the tetrahedrons BO_4 during amorphyzation of crystal copper metaborate.

We now try to present a possible scheme of conversion of the fraction of tetrahedral groups into trigonal ones. Figure 4*a* shows the crystalline structure of CuB_2O_4 and one of the metaborate rings comprising three tetrahedrons (Fig. 4*b*). Figure 4*c* shows the scheme of conversion of the tetrahedron into the triangle. We believe that if the B–O bond breaks, it most likely breaks where the B–O distance is maximum. Such distance in the CuB_2O_4 structure is equal to 1.48 Å and belongs to one of the three tetrahedrons. This oxygen atom belongs to the crystal bridge and participates in the exchange interaction through the Cu–O–B–O–Cu chain shown by the thick curve in Fig. 4*a*. For amorphous CuB_2O_4, the Cu–O–B–O–Cu bridge will be converted at least into a shorter Cu–O–B–O–Cu bridge, if for no other reason that the triangle has shorter B–O distances. This intensifies the exchange interaction [3]. It should be noted that only a fraction of the long Cu–O–B–O–Cu bridges is transformed into shorter ones. The remaining bridges in amorphous CuB_2O_4 most likely undergo small distortions, that is, their lengths and bonding angles of indirect exchange interaction change; this is confirmed by the NMR data. Moreover, the Cu–O–Cu bridges can be formed.

Thus, IR and NMR data have demonstrated that one third of the tetrahedral BO_4 groups is transformed into the BO_3 triangles during amorphyzation of CuB_2O_4. These structural changes intensify the exchange interactions and change the magnetic properties of amorphous CuB_2O_4.

Additional investigations, including neutron diffraction and muon spin relaxation analyses are required to identify the magnetic state of amorphous CuB_2O_4 below 8 K [3].

The authors would like to acknowledge A. N. Vtyurin, A. I. Pankrats, and O. A. Bayukov for interest to this work and useful discussions.

This work was supported in part by the Russian Foundation for Basic Research (grant No. 03-02-16701) and the Ministry of Education of the Russian Federation (grant E 02-3.4-227).

REFERENCES

1. G. A. Petrakovskii, K. A. Sablina, A. M. Vorotynov, *et al*., Zh. Eksp. Teor. Fiz., **98**, No. 4 (10), 1382–1389 (1990).
2. A. M. Vorotinov and K. A. Sablina, Solid State Commun., **87**, No. 3, 209–211 (1993).
3. L. V. Udod, K. A. Sablina, A. I. Pankrats, *et al*., Neorg. Mater., **39**, No. 11, 1356–1364 (2003).
4. S. Martynov, G. Petrakovskii, and B. Roessli, J. Mag. Mag. Mater., **269**, No. 1, 106 (2003).

5. M. Boehm, B. Roessli, *et al*., Phys. Rev., **B68**, 024405 (2003).
6. A. I. Pankrats, G. A. Petrakovskii, M. A. Popov, *et al*., Pis'ma Zh. Eksp. Teor. Fiz., **78**, No. 9, 1058–1062 (2003).
7. J. Krogh-Moe, Phys. Chem. Glasses, **6**, No. 2, 46–54 (1965).
8. G. E. Jellison, Jr. and P. J. Bray, J. Non-Cryst. Solids, **29**, No. 2, 187 (1978).
9. Koijnendijk, Philips Res. Rep., Suppl. 1, 123–181 (1975).
10. C. E. Weir and R. A. Schroeder, J. Res. Nat. Bur. Stand., **68A**, No. 5, 465–487 (1964).
11. G. A. Petrakovskii, K. A. Sablina, D. A. Velikanov, *et al*., Kristallografiya, **45**, No. 5, 926–929 (2000).
12. M. Martines-Ripoll, S. Martines-Carrera, and S. Garsia-Blanco, Acta Crystallogr., **B27**, No. 3, 677–681 (1971).
13. G. K. Abdulaev and Kh. S. Mamedov, Zh. Spektrosk. Khim., **22**, No. 4, 184–187 (1981).
14. B. N. Meera and J. Ramakrishna, J. Non-Cryst. Solids, **159**, 1–21 (1993).
15. Ezzeldin Metwalli, J. Non-Cryst. Solids, 2003, **317**, No. 3, 221–230 (1993).
16. M. Trunnell, D. R. Torgeson, S. W. Martin, and F. Borsa, J. Non-Cryst. Solids, **139**, 257–267 (1992).
17. P. J. Bray, J. Non-Cryst. Solids, **75**, Nos. 1–3, 29–36 (1985).